

BAND STRUCTURE MODEL AND OPTICAL PROPERTIES IN GRAPHITE ACCEPTOR COMPOUNDS

J. Blinowski*, Nguyen Hy Hau, C. Rigaux and J.P. Vieren
 Groupe de Physique des Solides de l'Ecole Normale Supérieure,
 24 rue Lhomond, 75231 Paris Cedex 05, France

The 2D band structure model for 1,2,3,4 charged graphite layers is presented. Optical reflectivity spectra for low stage graphite acceptor compounds are reported and interpreted within the model.

I. Band Structure Model

There exists striking experimental evidence of the 2D character of carriers in GAC [1]. We propose a 2D band structure model to describe electronic states in GAC. The nth stage compound is treated as a set of independent equivalent subsystems consisting of n charged graphite layers separated from each other by intercalated layers with the rigid distribution of the compensating charge. The potential energy fluctuations due to intercalants are neglected within the graphite subsystems. We determine the band structure near the U point, the corner of the 2D Brillouin zone. We neglect σ - π mixing, and we approximate the Bloch functions by linear combinations of the 2n tight binding functions built from atomic 2p_z orbitals $\phi_z(\vec{r})$ centered at the non equivalent sites A_i, B_i of the layer i [2] [3]. In this basis the approximate Hamiltonians for 1,2,3 layers are represented by the submatrices of the following matrix :

$$\begin{array}{cccccc}
 & A_1 & B_1 & A_2 & B_2 & A_3 & B_3 \\
 \begin{array}{l} A_1 \\ B_1 \\ A_2 \\ B_2 \\ A_3 \\ B_3 \end{array} & \left[\begin{array}{cccccc}
 \delta + \delta_1 & -x & \cdot & \gamma_1 & 0 & \cdot & 0 & 0 \\
 -x^* & \delta - \delta_1 & \cdot & 0 & 0 & \cdot & 0 & 0 \\
 \cdot & \cdot \\
 \gamma_1 & 0 & -\delta + \delta_2 & -x^* & \gamma_1 & 0 & 0 & 0 \\
 0 & 0 & -x & -\delta - \delta_2 & 0 & 0 & 0 & 0 \\
 \cdot & \cdot \\
 0 & 0 & \gamma_1 & 0 & \delta + \delta_1 & -x & 0 & 0 \\
 0 & 0 & 0 & 0 & -x^* & \delta - \delta_1 & 0 & 0
 \end{array} \right] & \begin{array}{l} \\ \\ \\ \\ \\ \\ \\ \\ \\ \end{array}
 \end{array}$$

with $\delta_1=0$ for one layer,
 $\delta_2=\delta_1$ for two layers.

The corresponding matrix for 4 layers can be constructed by analogy [3]. $x \approx 3/2 \gamma_0 b(k_x - ik_y)$ (\vec{k} is the 2D wavevector taken from the U point). $b = 1.42\text{\AA}$ is the nearest neighbour distance ; γ_0 and γ_1 are the dominant intra (A_i - B_i) and inter (A_i - A_{i+1}) layer resonance integrals respectively.

$2\delta = (E_{A_1} + E_{B_1} - E_{A_2} - E_{B_2})/2$; $2\delta_1 = E_{A_1} - E_{B_1}$; $2\delta_2 = E_{A_2} - E_{B_2}$, where $E_j = \int |\phi_z(\vec{r} - \vec{r}_j)|^2 V(\vec{r}) d^3r$ is the potential energy at the jth lattice site.

δ , δ_1 , δ_2 are related to the excess charge localized on atomic sites. The details of the calculations are presented elsewhere [2] [3]. It turns out that $2\delta_1$, $2\delta_2$ are negligible in the first approximation whereas 2δ , the potential energy difference between external and internal layers, cannot be neglected in any band struc-

* Permanent address : Institute of Theoretical Physics, University of Warsaw.

ture calculations. The energy band structure, calculated for low stages ($n \leq 4$), is sketched in Figure 1a, b, c, d.

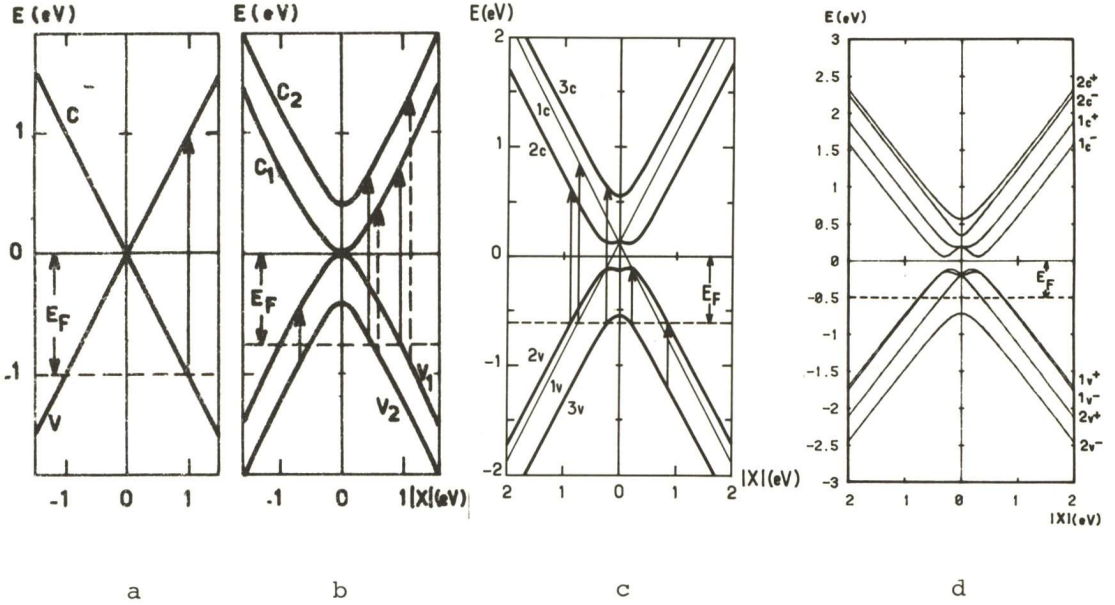


Figure 1 Band structure near the U point : a) stage 1, b) stage 2, c) stage 3 ($\delta = \gamma_1/3$), d) stage 4 ($\delta = \gamma_1/2$)

δ depends on the stage and is a function of the excess charge, i.e. of the charge transfer coefficient f . For stage 3, the δ -values for different charge transfer were established by self-consistent calculations of the excess charge distribution [3]. Near the U point, the dispersion relations for the valence and conduction bands are :

Stage 1 : $E_{C,V} = \pm |x|$

$$\text{Stage 2 : } \begin{cases} -E_{V1} = E_{C1} = -\gamma_1/2 + \sqrt{(\gamma_1/2)^2 + |x|^2} \\ -E_{V2} = E_{C2} = \gamma_1/2 + \sqrt{(\gamma_1/2)^2 + |x|^2} \end{cases}$$

$$\text{Stage 3 : } \begin{cases} E_1^{C,V} = \delta \pm |x| \\ E_2^{C,V} = \pm(\delta^2 + \gamma_1^2 + |x|^2 - \sqrt{\gamma_1^4 + (4\delta^2 + 2\gamma_1^2)|x|^2})^{1/2} \\ E_3^{C,V} = \pm(\delta^2 + \gamma_1^2 + |x|^2 + \sqrt{\gamma_1^4 + (4\delta^2 + 2\gamma_1^2)|x|^2})^{1/2} \end{cases}$$

II. Optical Properties

Low stages GAC exhibit metallic reflectance. Well-pronounced plasma edges depending on stage are observed in the near IR and visible region [2,4,5,6,10]. Figure 2 shows reflectivity spectra of stages 2,3,4 of AlCl₃-graphite. The position of the plasma minima shifts to lower energies with increasing stage number. Below the plasma edges, reflectivity spectra show the existence of stage-specific structures whose energies depend slightly on the nature of intercalate species [7] : they are observed (Fig.2) at $\hbar\omega = 0.37$ eV for stage 2,

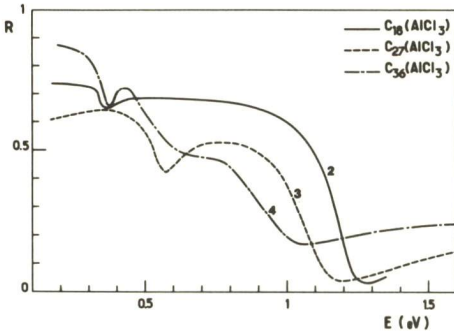


Figure 2. Reflectance spectra of stages 2, 3, 4 of AlCl₃-graphite

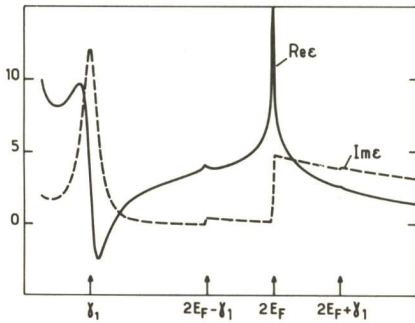


Figure 3. Frequency dependence of the real and imaginary parts of $\epsilon_{inter}(\omega)$ (stage 2)

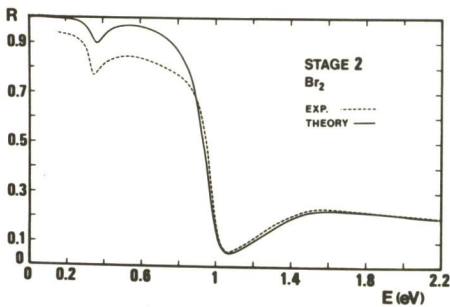


Figure 4. Comparison between theory and experiments

between 0.5 and 0.6eV for stage 3, at $\hbar\omega = 0.37$ and near 0.7eV in stage 4. Such features do not exist in first stage.

The reflectance data of GAC differ considerably from the spectrum of pristine graphite which presents a monotonic decrease between 0.3 and 1.8eV [8], the frequency dependence of $R(\omega)$ resulting almost exclusively from strong interband transitions in this spectral region. The observation of well-pronounced plasma edges in GAC implies that the thresholds of IB transitions occur at higher energies.

Optical reflectance data obtained on various GAC in the region 0.1-2.5eV are quantitatively interpreted within the framework of the 2D band structure model of "Graphite Independent Subsystems".

1) The frequency dependent dielectric function $\epsilon_{\perp}(\omega)$ was calculated for stages 1 and 2. The details of the calculations are reported in [2]. The model predicts the existence of important contributions to the dielectric function originating from strong valence to conduction transitions. These transitions begin at $\hbar\omega = 2E_F$ for stage 1 (Fig.1a) and at $\hbar\omega = 2E_F$ ($v_2 \rightarrow c_2, v_1 \rightarrow c_1$ transitions), $\hbar\omega = 2E_F + \gamma_1$ ($v_2 \rightarrow c_1, v_1 \rightarrow c_2$ transitions) for stage 2. (Fig.1b). Each threshold is characterized by a peak in $Re \epsilon_{inter}(\omega)$ and a step in $Im \epsilon_{inter}(\omega)$ which are shown in Fig.3, for stage 2.

The intraband contribution is proportional to the hole Fermi energy E_F and exhibits an unusual hole concentration dependence ($\epsilon_{intra} \propto N^{1/2}$). The total dielectric function $\epsilon(\omega)$ depends on E_F , an adjustable parameter, and $\gamma_1 = 0.377eV$. Two damping parameters, T_{eff} and τ , are also introduced to phenomenologically account for the carrier scattering in inter- and intraband terms respectively. The comparison between theory and experiments is reported in Figure 4 for stage 2 of Br₂-graphite. The position of the minimum depends drastically on E_F which enters into both ϵ_{intra} and ϵ_{inter} .

At $\hbar\omega > 2E_F$, the important interband contribution to $Im \epsilon(\omega)$ drastically influences the frequency dependence of $R(\omega)$, which presents a slow decrease in the high frequency region,

similarly as in the case of pure graphite. From the theoretical fits (Fig.4), we determine E_F and consequently the charge transfer coefficient ($E_F = \gamma_0 \sqrt{\pi f \sqrt{3}/2\ell}$) for several compounds $C_{2\ell}A$ of stage 2. Numerical values are listed in Table 1. The lower and upper limits of f correspond to $\gamma_0 = 3.12\text{eV}$ [9] and 2.4eV respectively.

GAC	$C_{16}Br_2$	$C_{16}ICl$	$C_{24}SbCl_5$	$C_{18}AlCl_3$	$C_{16}AsF_5$
E_F (eV)	0.70	0.75	0.75	0.90	1
f	0.15-0.25	0.17-0.29	0.25-0.44	0.27-0.47	0.30-0.51

Table 1

2) The stage-characteristic structures observed in the near IR region [7] [10] provide evidence of the intervalence transitions (IVT) predicted by the model: Stage 2 : $v_2 \rightarrow v_1$ transitions are expected at $\hbar\omega = \gamma_1$ (Fig.1b). Using a Lorentzian function to remove the singularity of $\epsilon_{inter}(\omega)$ at $\hbar\omega = \gamma_1$, the calculated reflectance interprets quite well the position and the lineshape of the structure (Fig.4), systematically observed at 0.37eV in all GAC of stage 2. Stage 3 : Strong intervalence $v_3 \rightarrow v_2$ transitions are predicted (Fig.1c) : For $\delta=0$, the corresponding absorption peak should appear at $\hbar\omega = \sqrt{2}\gamma_1 = 0.53\text{eV}$. Due to the modification of the energy bands induced by electrostatic effects, the IVT ($v_3 \rightarrow v_2$) give rise to an absorption band in the spectral region : $\sqrt{2}\gamma_1^2 + \delta^2 - \delta < \hbar\omega < \sqrt{2}\gamma_1^2 + 4\delta^2$. The δ -values were estimated from the self-consistent procedure by assuming the same charge transfer in stages 2 and 3 ($\delta = 0.12-0.14\text{eV}$ for Br_2 ; $0.15-0.19\text{eV}$ for $AlCl_3$). The corresponding energy region for the $v_3 \rightarrow v_2$ transitions is in good agreement with the experimental position of the strong reflectance structure observed near $0.5-0.6\text{eV}$ in various GAC [7]. (Fig.2). Stage 4 : In the case $\delta = 0$, the allowed IVT are $2v^- \rightarrow 1v^+$ and $2v^+ \rightarrow 1v^-$ at $\hbar\omega = \frac{\sqrt{5}+1}{2} \gamma_1$. For $\delta \neq 0$, all IVT are allowed for any k . One can still however expect two strong transitions $2v^- \rightarrow 1v^+$ and $2v^+ \rightarrow 1v^-$ between the nearly parallel valence bands with the final states above E_F (Fig.1d). The value of $\delta = \gamma_1/2$ accounts for the position of the reflectivity structures observed at 0.37 and 0.74eV [7] [10]. The observation of the IVT in stages 2,3,4 of various AC constituents (Fig.2) a strong experimental support for the applicability of our band structure model to GAC.

References

- 1) I. Rosenman, F. Batallan, G. Furdin: Phys. Rev. B20 (1979) 2373.
C. Simon, F. Batallan, I. Rosenman, H. Fuzellier: Phys. Rev. (in press).
- 2) J. Blinowski, Nguyen Hy Hau, C. Rigaux, J.P. Vieren, R. Le Toullec, G. Furdin, A. Hérold, J. Melin: Journal de Physique 41 (1980) 47.
- 3) J. Blinowski, C. Rigaux: Journal de Physique 41 (1980) 667 and International Conference on Intercalation Compounds of Graphite, Provincetown, 1980. To be published in Synthetic Metals.
- 4) J.E. Fischer, T.E. Thompson, G.M. Foley, D. Guérard, M. Hoke, F.L. Lederman: Phys. Rev. Lett. 37 (1976) 769.
- 5) T.E. Thompson, E.R. Falardeau, L.R. Hanlon: Carbon 15 (1977) 39.
- 6) L.R. Hanlon, E.R. Falardeau, D. Guérard, J.E. Fischer: Materials Science and Engineering 31 (1977) 161.
- 7) Nguyen Hy Hau, J. Blinowski, C. Rigaux, R. Le Toullec, G. Furdin, A. Hérold, R. Vangelisti: 2nd International Conference on Intercalation Compounds of Graphite, Provincetown (1980). To be published in Synthetic Metals.
- 8) E.A. Taft, H.R. Philipp: Phys. Rev. 138 (1965) A 197.
- 9) M.S. Dresselhaus, G. Dresselhaus, J.E. Fischer: Phys. Rev. B15 (1977) 3180.
- 10) P.C. Eklund, D.S. Smith, V.R.K. Murthy: 2nd International Conference on Intercalation Compounds of Graphite, Provincetown (1980). To be published in Synthetic Metals.